

# Distributed Collision-Free Bearing Coordination of Multi-UAV Systems with Actuator Faults and Time Delays

Kefan Wu, Junyan Hu, Zhenhong Li, Zhengtao Ding, and Farshad Arvin

**Abstract**—Coordination of unmanned aerial vehicle (UAV) systems has received great attention from robotics and control communities. In this paper, we investigate the distributed formation tracking problem in heterogeneous nonlinear multi-UAV networks via bearing measurements. Firstly, a novel bearing-only protocol is designed for follower agents to achieve the desired formation. Particularly, we establish a compensation function on the basis of bearing measurements to deal with the nonlinearity and actuator faults in the agent dynamics. The stability of the proposed strategy can be ensured by Lyapunov method in the presence of certain time delays. Moreover, to ensure safe operation in real-world scenarios, we extend the protocol and propose a sufficient condition to avoid potential collisions among the agents. The robustness of the collision-free controller with continuous action is also considered in the protocol design. Finally, the simulation case studies are presented to validate the feasibility of the theoretical results.

**Index Terms**—Bearing coordination, actuator faults, collision-free, time delays, multi-UAV networks.

## I. INTRODUCTION

IN recent years, planning and control of unmanned aerial vehicle (UAV) systems has been a hot research topic in the field of intelligent transportation systems (ITS). Multi-UAV networks refer to systems composed of a group of networked drones that collaborate and communicate with each other to accomplish various tasks. Each UAV operates as an autonomous agent, capable of making decisions and taking actions based on its onboard sensors, communication capabilities, and assigned tasks, which have the potential to revolutionize a wide range of applications, such as surveillance [1], area coverage [2], search and rescue [3], etc. Compared with single drone, multi-UAV networks can be deployed to cover a larger area with high efficiency. More comprehensive data is able to be collected and analysed during the mission. However, quite a few issues are still waiting to be resolved when applying coordination techniques to complex real-world multi-UAV networks, under some practical constraints including actuator faults, time delays, collisions, nonlinear and heterogeneous dynamics, etc.

Formation tracking, as one of the most fundamental coordination methods, has been used extensively in multi-agent

systems (MAS), e.g. vehicle platooning [4], [5], ecosystem hacking using micro-robot swarms [6], trajectory tracking and navigation [7], [8], collaborative manipulation [9], [10], etc. A traditional and straightforward way to tackle multi-agent formation problem is to take the advantage of the position information of each agent. For instance, in [11], a leader-follower position-based formation was proposed via prescribed performance method. The authors in [12] proposed a novel formation-containment protocol based on semi-definite programming. The time-varying adaptive formation tracking problem was considered in [13], where the system is high-order, nonlinear, and stochastic. In [14], a finite-time formation strategy was implemented to ITS on the basis of recurrent neural network (RNN). The author in [15] discussed the formation tracking problem of nonlinear ITS with random disturbances. All the agents are able to keep the target formation under the event-trigger scheme. In the works mentioned above, the position information of the agents plays an important role in solving the problem of achieving the target formation. Another standard approach to deal with the formation problem is through distance measurements. Mehdifar et al. [16] provided a novel formation protocol by distance measurement for MAS with exogenous disturbance. In another work, Babazadeh et al. discussed the distance-based formation problem with energy constraint in [17]. Both the optimal control method and state-dependent Riccati equation approach were utilized in this work. However, by using the aforementioned methods, the formation tracking performance of the MAS will not be satisfactory if the state or distance information is difficult to be obtained in some extreme environmental conditions.

To deal with these restrictions, the research on bearing-only formation protocol has gained considerable attention ([18]–[23]), where only the relative bearing information is available among neighboring agents. In contrast to the position-based and distance-based methods, the bearing measurements only require the angle observation which can be obtained directly from vision-based sensors during the hardware implementations [24]. The authors in [25] proposed the bearing rigidity theorem in 2D space to guarantee the uniqueness of the configuration generated by bearing vectors. Zhao et al. further extended the bearing rigidity theorem to arbitrary dimensions in [26]. In [27], a bearing-only protocol was designed for heterogeneous MAS with an adaptive scheme. The leader-follower bearing-only formation issues for double-integrator systems with local reference frames were investigated in [28], where the velocities of the leaders are constant. Another main problem in bearing-

The presented work was partially supported by EU-H2020-FET-OPEN RoboRoyale project, grant agreement No. 964492.

K. Wu, Z. Li and Z. Ding are with the Department of Electrical and Electronic Engineering, The University of Manchester, Manchester, M13 9PL, U.K. (e-mail: {kefan.wu; zhenhong.li; zhengtao.ding}@manchester.ac.uk)

J. Hu and F. Arvin are with Department of Computer Science, Durham University, Durham, DH1 3LE, U.K. (e-mail: {junyan.hu; farshad.arvin}@durham.ac.uk)

only formation research is how to avoid collisions between each agent during the formation to ensure that the bearing vectors are well-defined. A finite-time bearing-only formation protocol with collision avoidance was proposed in [29] to deal with heterogeneous multi-robot platforms. However, in the aforementioned works, the dynamics of each agent are relatively ideal and simple, which may not be accurate enough to mimic the dynamics of real-world agents (e.g., drones, robots, vehicles, etc.). There is still an open gap for handling bearing-only formation problems in a system with complex and nonlinear dynamics.

It is noticeable that there also exist many significant indicators to affect the stability of the MAS such as time delays and actuator faults. Time delay often exists in practical systems and it should be considered when establishing the formation control law. In [30], a containment strategy was designed for double-integrator MAS with time-varying delays. The authors in [31] provided a neuro-adaptive formation tracking protocol for second-order MAS with time delays. In [32], the communication delays were taken into account to deal with the formation problem for the multiple UAV systems. When it comes to handling the actuator faults in the controller, the authors in [33] studied the fault-tolerant formation problem in double-integrator systems with directed communication. An adaptive approach was implemented in the controller to deal with the failures. In [34], a fault-tolerant formation protocol was introduced for heterogeneous UAVs with reinforcement learning. Yu et al. in [35] employed an adaptive scheme in the formation-containment controller to tackle the actuator faults in networked unmanned airships. However, in the above research, the bearing-only techniques were not taken into consideration. Consequently, it is desirable to establish a bearing-only protocol to deal with actuator faults and time delays in nonlinear MAS.

In this research, we address the fault-tolerant bearing coordination problems for heterogeneous nonlinear multi-UAV networks. To deal with the unknown nonlinear item and the actuator faults, a designed compensation scheme is applied in the controller to achieve a better performance than the traditional bearing-only protocols. Moreover, we design the compensation function and present a condition to avoid collisions among the agents during the formation task. The main contributions of this article can be summarized as follows:

- A distributed fault-tolerant coordination protocol is designed for heterogeneous nonlinear multi-UAV networks by only detecting the relative bearing information. In contrary to the conventional position-based and distance-based protocols, the proposed algorithm is able to reduce the sensing requirements of each agent significantly as the angle observation can be easily obtained from vision-based sensors.
- A novel compensation function based only on bearing measurements is included to deal with the nonlinear dynamics in the system and the actuator faults in the controller. The stability of the bearing-only protocol is established by Lyapunov method. Furthermore, we also provide the robustness analysis of the protocol in the presence of certain time delays.
- Collision-avoidance is considered in the algorithm design.

We reconstruct a compensation function and provide a sufficient condition to ensure that there is no collision between each neighboring agent during the formation task. Moreover, we improve the form of the compensation function to a continuous action and discuss the robustness of the continuous formation protocol.

## II. PRELIMINARIES AND PROBLEM STATEMENT

### A. Notations and Preliminaries

Consider a team of  $N$  networked drones (with  $N_l$  leaders and  $N_f$  followers) in  $\mathbb{R}^d$  ( $N \geq 2$ ,  $d \geq 2$  and  $N_l + N_f = N$ ). The interaction among the agents is described by an undirected graph  $\mathcal{G} = (\mathcal{V}, \mathcal{E})$  with a nonempty vertex set  $\mathcal{V} = \mathcal{V}_l \cup \mathcal{V}_f = \{v_1, \dots, v_N\}$  and an edge set  $\mathcal{E} \subseteq \mathcal{V} \times \mathcal{V}$ , where  $\mathcal{V}_l = \{v_1, \dots, v_{N_l}\}$  and  $\mathcal{V}_f = \{v_{N_l+1}, \dots, v_N\}$  represent the set of leaders and followers. The edge  $(i, j) \in \mathcal{E}$  demonstrates that agent  $i$  can measure the relative bearing of agent  $j$ , and hence agent  $j$  is a neighbor of  $i$ . Denote  $\mathcal{N}_i = \{j \in \mathcal{V} : (i, j) \in \mathcal{E}\}$  as the set of neighbors of agent  $i$ . It can be obtained that  $(i, j) \in \mathcal{E} \Leftrightarrow (j, i) \in \mathcal{E}$  because the graph  $\mathcal{G}$  is undirected.

Define the position of the  $i^{\text{th}}$  agent as  $p_i \in \mathbb{R}^d$ . Suppose the edge  $(i, j)$  corresponds to the  $k^{\text{th}}$  directed edge in oriented graph where  $k \in \{1, \dots, M\}$ . The *edge vector*  $\eta_{ij}$  for edge  $(i, j)$  can be defined as

$$\eta_{ij} = \eta_k = p_j - p_i.$$

Hence, the relative *bearing vector* of the  $j^{\text{th}}$  agent with respect to the  $i^{\text{th}}$  agent is given as

$$\beta_{ij} = \beta_k = \frac{p_j - p_i}{\|p_j - p_i\|},$$

where  $\|\cdot\|$  denotes the Euclidean norm of a vector or the spectral norm of a matrix. The unit vector  $\beta_{ij}$  represents the relative bearing of  $p_j$  with respect to  $p_i$ .

An oriented graph is an undirected graph with an orientation, which is widely used in this paper. An orientation of an undirected graph is the assignment of a direction to each edge. Denote  $M = |\mathcal{E}|$  as the number of undirected edges. Then, the incidence matrix of the oriented graph is denoted as  $H \in \mathbb{R}^{M \times N}$ , where  $[H]_{ki} = 1$  if vertex  $i$  is the head of edge  $k$ ;  $[H]_{ki} = -1$  if vertex  $i$  is the tail of edge  $k$ ; and  $[H]_{ki} = 0$  otherwise. For an undirected connected graph, it holds that  $\text{rank}(H) = N - 1$  and  $H\mathbf{1}_N = 0$  [36]. Let  $p = [p_1^T, \dots, p_N^T]^T$ ,  $\eta = [\eta_1^T, \dots, \eta_M^T]^T$ , and  $\beta = [\beta_1^T, \dots, \beta_M^T]^T$ . Denote  $I_d \in \mathbb{R}^{d \times d}$  as the identity matrix, it can be implied from the definition of  $H$  that  $\eta = \bar{H}p$ , where  $\bar{H} = H \otimes I_d$ .

Define the scale of the formation as

$$S(t) = \sqrt{\frac{1}{N} \sum_{i=1}^N \|p_i - \bar{p}\|^2} = \frac{\|p - \mathbf{1}_N \otimes \bar{p}\|}{\sqrt{N}},$$

where  $\bar{p} = \frac{1}{N}(\mathbf{1}_N \otimes I_d)^T p$  denotes the centroid of the formation.

Denote  $p^* = [p_1^{*T}, \dots, p_N^{*T}]^T$  and  $\beta^* = [\beta_1^{*T}, \dots, \beta_M^{*T}]^T$  as the configuration and bearing vector of the target formation. The *bearing Laplacian matrix*  $\mathcal{B} \in \mathbb{R}^{dN \times dN}$  is demonstrated

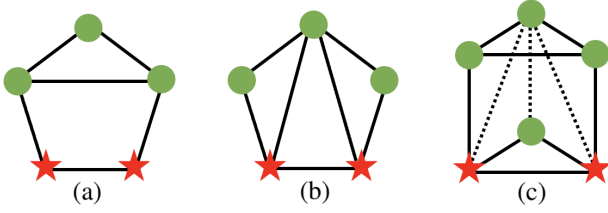


Fig. 1. Non-unique target formation under connections (a), and unique target formation under connections (b and c).

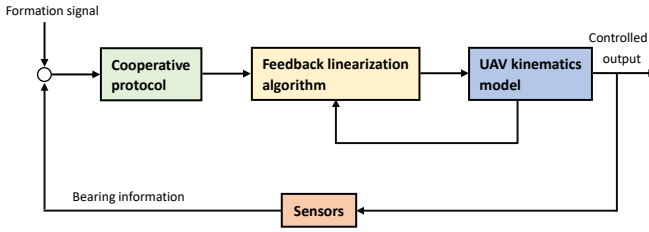


Fig. 2. The control architecture associated with the UAV systems.

to characterize the properties of a formation. Let  $P_{\beta_{ij}^*} = I_d - \beta_{ij}^* (\beta_{ij}^*)^T \in \mathbb{R}^{d \times d}$ . The block of  $\mathcal{B}$  is expressed as [37]

$$[\mathcal{B}(\mathcal{G}, p)]_{ij} = \begin{cases} \mathbf{0}, & i \neq j, (i, j) \notin \mathcal{E}, \\ -P_{\beta_{ij}^*}, & i \neq j, (i, j) \in \mathcal{E}, \\ \sum_{k \in \mathcal{N}_i} P_{\beta_{ik}^*}, & i = j, i \in \mathcal{V}. \end{cases}$$

It is obvious that  $\mathcal{B}$  is semi-positive definite, and  $\mathcal{B}p^* = \mathcal{B}(\mathbf{1}_N \otimes I_d) = \mathbf{0}$ . According to the description of  $H$  and  $\mathcal{B}$ , we can imply that

$$\mathcal{B} = \bar{H}^T \text{diag}(P_{\beta_k^*}) \bar{H}, \quad (1)$$

The partition of the bearing Laplacian matrix can be expressed as

$$\mathcal{B} = \begin{bmatrix} \mathcal{B}_{ll} & \mathcal{B}_{lf} \\ \mathcal{B}_{lf}^T & \mathcal{B}_{ff} \end{bmatrix}, \quad (2)$$

where  $\mathcal{B}_{ff} \in \mathbb{R}^{dN_f \times dN_f}$ . The uniqueness of the target formation can be ensured by the following lemma.

**Lemma 1.** [37] *The target formation  $\{p_i^*\}_{i \in \mathcal{V}}$  can be uniquely determined by the states of the leaders  $\{p_i^*\}_{i \in \mathcal{V}_l}$  and the bearing vectors  $\{\beta_{ij}^*\}_{(i,j) \in \mathcal{E}} \Leftrightarrow \mathcal{B}_{ff}$  is non-singular.*

It should be noticed from Lemma 1 that the uniqueness of the target formation depends on the sub-matrix  $\mathcal{B}_{ff}$ , which denotes the connections between each follower agent. For better understanding, three examples are listed in Fig. 1, where the leaders are denoted by red stars, and the followers are marked by green circles. The target formation can be uniquely determined by the bearing vectors and the position of the leaders under the topology (b) and (c).

## B. Problem Statement

In this paper, we focus on constructing cooperative bearing-only formation strategies for the followers in multi-UAV systems. Let  $p_i = [p_{ix}, p_{iy}, p_{iz}]^T$  be the state of the  $i^{\text{th}}$  UAV

in a 3D space. Define  $\chi_i$  and  $\gamma_i$  as the yaw and pitch angles of the  $i^{\text{th}}$  UAV to determine the velocity orientation of each agent. The kinematic model of the  $i^{\text{th}}$  UAV is described as

$$\begin{aligned} \dot{p}_{ix} &= v_i \cos \chi_i \cos \gamma_i \\ \dot{p}_{iy} &= v_i \cos \chi_i \sin \gamma_i \\ \dot{p}_{iz} &= v_i \sin \chi_i \\ \dot{\chi}_i &= \omega_{\chi_i} \\ \dot{\gamma}_i &= \omega_{\gamma_i} \end{aligned} \quad (3)$$

where  $v_i$ ,  $\omega_{\chi_i}$ ,  $\omega_{\gamma_i}$  stand for the linear and angular velocities. Based on the fact that the attitude dynamics of the drone is faster than the translation dynamics [38]. The feedback linearization technique [39] can be utilized to transfer the highly complex UAV kinematic model (3) to a first-order system [38]. Hence, the dynamics of each follower UAV can be described as

$$\dot{p}_i(t) = u_i^f(t) + \phi_i(p_i(t)), \quad \forall i \in \mathcal{V}_f. \quad (4)$$

where  $\phi_i(\cdot) \in \mathbb{R}^d$  denotes the unknown nonlinear function in the system,  $u_i^f(t) \in \mathbb{R}^d$  stands for the control input with the actuator faults caused by control system failures for the  $i^{\text{th}}$  agent [40], which is described as

$$u_i^f(t) = u_i(t) + f_i(t), \quad (5)$$

where  $u_i(t) \in \mathbb{R}^d$  is the control input. The actuator faults  $f_i(t) \in \mathbb{R}^d$  represent the unknown output bias of the actuator channel ([41], [42]) in the controller for the  $i^{\text{th}}$  agent. Fig. 2 reveals the overall control architecture. The bearing-only protocol designed later will be implemented as the control input.

Substituting (5) into (4), the dynamics of the heterogeneous multi-UAV systems with actuator faults is written as

$$\dot{p}_i(t) = u_i(t) + f_i(t) + \phi_i(p_i(t)), \quad \forall i \in \mathcal{V}_f. \quad (6)$$

**Remark 1.** *In this work, we mainly focus on developing a novel bearing-based formation tracking strategy to address multi-UAV coordination problems. One of the challenges is to deal with the collective behaviors of the UAVs using only relative bearing information instead of absolute positions. Hence, only simplified UAV models are considered in the coordination protocol design to ensure that a feasible and effective solution can be obtained, following other important works in this field (e.g., [43]–[46]). Considering that the simplified UAV model may not be precise enough in some real-world implementations, a fine-tuning of the low-level feedback linearization controller is suggested to be done before applying the proposed high-level coordination approach.*

To achieve the desired formation tracking objective, we have the following assumptions

*Assumption 1:* The unknown nonlinear function  $\phi_i(\cdot)$  is upper-bounded. i.e.,

$$\|\phi_i(\cdot)\| \leq \tilde{\phi}(t), \quad (7)$$

where  $\tilde{\phi}(t)$  is a known continuous function.

*Assumption 2:* The unknown actuator fault  $f_i(t)$  is upper-

bounded. i.e.,

$$\|f_i(t)\| \leq \tilde{f}, \quad (8)$$

where  $\tilde{f}$  is a known positive constant.

*Assumption 3:* The target formation can be uniquely determined by the positions of the leaders., i.e.,  $\mathcal{B}_{ff} > 0$ .

*Assumption 4:* There is no collision between each agent during the formation task., i.e. There exists  $c > 0$ , such that  $\|\eta_{ij}\| > c, \forall i, j \in \mathcal{V}$

*Assumption 5:* The formation scale  $\mathcal{S}(t)$  is upper-bounded during the task. i.e.,  $\mathcal{S}(t) \leq \mathcal{S}_0, \forall t \geq 0$ .

We now illustrate the main objectives of this paper in a precise form. Suppose the dynamics of each agent with actuator faults can be generalized by system (6). The following problems are solved in this work: i) How to design the fault-tolerant formation protocol for heterogeneous nonlinear multi-UAV networks based merely on the bearing vectors  $\{\beta_{ij}\}_{(i,j) \in \mathcal{E}}$ . ii) How is the stability of the proposed strategy for heterogeneous nonlinear time delay systems. iii) How to improve the control scheme to avoid collisions between each agent. iv) How to develop the collision-free controller with continuous action.

### III. FAULT-TOLERANT BEARING FORMATION PROTOCOLS

In this section, a fault-tolerant bearing-only protocol is proposed for heterogeneous nonlinear multi-UAV networks. Moreover, we provide the stability analysis of the controller in the presence of time delays and actuator faults.

#### A. Bearing-only protocol design for followers

The bearing-only control protocol of the followers is designed as

$$u_i(t) = k_f \sum_{j \in \mathcal{N}_i} \zeta_{ij} + \sum_{j \in \mathcal{N}_i} \Phi_i(\zeta_{ij}), \quad i \in \mathcal{V}_f. \quad (9)$$

where  $\zeta_{ij} = \zeta_k = \beta_{ij}(t) - \beta_{ij}^*(t)$  denotes the bearing error of the  $k^{\text{th}}$  bearing vector,  $k_f$  is the positive control gain which should be designed later, and the compensation function is designed as

$$\Phi_i(\zeta_{ij}) = \begin{cases} R(t) \frac{\zeta_{ij}}{\|\zeta_{ij}\|^2}, & \text{when } \|\zeta_{ij}\| \neq 0 \\ 0, & \text{when } \|\zeta_{ij}\| = 0. \end{cases}$$

where

$$R(t) = \tilde{\phi}^2(t) + \tilde{f}^2. \quad (10)$$

It can be found that the compensation function is only based on bearing measurements.

**Remark 2.** It can be observed that the compensation function  $\Phi_i(\zeta_{ij})$  is designed merely based on bearing measurement. Hence, the overall controller (9) is still bearing-only, which is more feasible in some real applications if traditional position or distance measurements are not available or are less accurate (e.g, the sensor is low-cost). Moreover, protocol (9) is distributed because we only use the relative bearing vectors from its neighbors  $\mathcal{N}_i$  for the  $i^{\text{th}}$  UAV via a communication network.

Define the formation error as  $\xi_i = p_i - p_i^*$ , and  $\xi = [0, \xi_f^T]^T$ , where  $\xi_f = [\xi_{N_i+1}^T, \dots, \xi_N^T]^T$ . Let  $\zeta = [\zeta_1^T, \dots, \zeta_M^T]^T = g - g^*$ . Before we show the main theorem and associate proof, the following lemmas should be introduced

**Lemma 2.** [47]: Suppose Assumption 4 holds, we have

$$p^T \bar{H}^T \zeta \geq 0 \quad (11)$$

$$(p^*)^T \bar{H}^T \zeta \leq 0 \quad (12)$$

$$\xi^T \bar{H}^T \zeta \geq 0 \quad (13)$$

**Lemma 3.** For each agent in the system, under Assumptions 4 and 5, it holds that

$$\|\eta_k\| \leq 2N\mathcal{S}_0. \quad (14)$$

*Proof.* Since

$$\begin{aligned} N^2 \mathcal{S}(t)^2 &= N \sum_{k=1}^N \|p_k - \bar{p}\|^2 \\ &\geq (\|p_i - \bar{p}\| + \sum_{k \in \mathcal{V}, k \neq i} \|p_k - \bar{p}\|)^2 \\ &\geq \|p_i - \bar{p}\|^2 \end{aligned} \quad (15)$$

From Assumption 5, we have

$$\begin{aligned} \|\eta_k\| &= \|p_i - p_j\| \\ &= \|(p_i - \bar{p}) - (p_j - \bar{p})\| \\ &\leq \|p_i - \bar{p}\| + \|p_j - \bar{p}\| \\ &\leq 2N\mathcal{S}(t) \leq 2N\mathcal{S}_0. \end{aligned} \quad (16)$$

□

**Lemma 4.** Suppose Assumptions 4 and 5 hold, we have

$$p^T \bar{H}^T \zeta \geq \frac{\xi^T \xi \lambda_{\min}(\mathcal{B}_{ff})}{4N\mathcal{S}_0}, \quad (17)$$

where  $\lambda_{\min}(\mathcal{B}_{ff}) > 0$  denotes the minimum eigenvalue of  $\mathcal{B}_{ff}$ .

*Proof.* In one hand, based on Lemma 3 in [47], it can be obtained that

$$\begin{aligned} p^T \mathcal{B} p &= \sum_{k=1}^M \|\eta_k\|^2 (1 - \beta_k^T \beta_k^*) (1 + \beta_k^T \beta_k^*) \\ &\leq 2 \sum_{k=1}^M \|\eta_k\|^2 (1 - \beta_k^T \beta_k^*) \\ &= \sum_{k=1}^M \|\eta_k\|^2 \|\beta_k - \beta_k^*\|^2. \end{aligned} \quad (18)$$

In another hand, it can be computed that

$$\begin{aligned} p^T \bar{H}^T \zeta &= \sum_{k=1}^M (\eta_k^T \beta_k - \eta_k^T \beta_k^*) \\ &= \sum_{k=1}^M \|\eta_k\| (1 - \beta_k^T \beta_k^*). \end{aligned} \quad (19)$$

Furthermore, let  $\xi_f = [\xi_{N_i+1}^T, \dots, \xi_N^T]^T$ , and  $\xi$  can be

rewritten as

$$\xi = [0, \xi_f^T]^T. \quad (20)$$

Since  $\mathcal{B}p^* = 0$ , it follows that

$$p^T \mathcal{B}p = \xi^T \mathcal{B}\xi = \xi_f^T \mathcal{B}_{ff} \xi_f \geq \xi^T \xi \lambda_{\min}(\mathcal{B}_{ff}) \quad (21)$$

Combining (14), (18), (19), and (21), we have

$$\begin{aligned} \xi^T \xi \lambda_{\min}(\mathcal{B}_{ff}) &\leq p^T \mathcal{B}p \\ &\leq 2 \sum_{k=1}^M \|\eta_k\|^2 (1 - \beta_k^T \beta_k^*) \\ &\leq 2 \max_k \|\eta_k\| \sum_{k=1}^M \|\eta_k\| (1 - \beta_k^T \beta_k^*) \quad (22) \\ &\leq 4N\mathcal{S}_0 \sum_{k=1}^M \|\eta_k\| (1 - \beta_k^T \beta_k^*) \\ &= 4N\mathcal{S}_0 p^T \bar{H}^T \zeta. \end{aligned}$$

Hence, we can claim that (17) holds.  $\square$

Now, we would like to present the following theorem.

**Theorem 1.** *Consider the heterogeneous nonlinear leader-follower multi-UAV systems (6). Under Assumptions 1-5 and the control strategy (9), all the agents will converge to the target formation exponentially if  $k_f$  is selected to satisfy*

$$k_f > \frac{4NN_f\mathcal{S}_0}{\lambda_{\min}(\mathcal{B}_{ff})Mc}. \quad (23)$$

*Proof.* By implementing the protocol (9), the dynamics of the nonlinear multi-UAV systems (6) can be written in a compact form as

$$\dot{p} = - \begin{bmatrix} 0 & 0 \\ 0 & I_{dN_f} \end{bmatrix} \bar{H}^T (k_f \zeta + \Phi(\zeta)) + \phi(p(t)) + f(t), \quad (24)$$

where  $\phi(p(t)) = [0, \dots, \phi_{N_i+1}^T(p_{N_i+1}(t)), \dots, \phi_N^T(p_N(t))]^T$ ,  $f(t) = [0, \dots, f_{N_i+1}^T(t), \dots, f_N^T(t)]^T$ , and

$$\Phi(\zeta) = R(t) \left[ \frac{\zeta_1^T}{\|\zeta_1\|^2}, \dots, \frac{\zeta_M^T}{\|\zeta_M\|^2} \right]^T.$$

The Lyapunov candidate can be selected as

$$V = \frac{1}{2} \xi^T \xi. \quad (25)$$

Based on Lemma 2 and Lemma 4, the deviation of  $V$  can be expressed as

$$\begin{aligned} \dot{V} &= \xi^T \dot{p} \\ &= -k_f \xi^T \bar{H}^T \zeta - \xi^T \bar{H}^T \Phi(\zeta) + \xi^T (\phi(p(t)) + f(t)) \\ &\leq -k_f p^T \bar{H}^T \zeta - \xi^T \bar{H}^T \Phi(\zeta) + \xi^T (\phi(p(t)) + f(t)) \quad (26) \\ &\leq -k_f \frac{\xi^T \xi \lambda_{\min}(\mathcal{B}_{ff})}{4N\mathcal{S}_0} + \Pi, \end{aligned}$$

where

$$\Pi = -\xi^T (\bar{H}^T \Phi(\zeta) - \phi(p(t)) - f(t)).$$

According to (7), (8), and the average inequality, we can imply

that

$$\begin{aligned} \Pi &= -(\eta - \eta^*)^T \Phi(\zeta) + \xi^T (\phi(p(t)) + f(t)) \\ &= -\left( \sum_{k=1}^M \frac{\eta_k^T \beta_k - \eta_k^* \beta_k^*}{\|\beta_k - \beta_k^*\|^2} - \sum_{k=1}^M \frac{\eta_k^{*T} \beta_k - \eta_k^* \beta_k^*}{\|\beta_k - \beta_k^*\|^2} \right) (\tilde{\phi}^2(t) + \tilde{f}^2) \\ &\quad + \xi^T (\phi(p(t)) + f(t)) \\ &= -\left( \sum_{k=1}^M \frac{\|\eta_k\| (1 - \beta_k^T \beta_k^*)}{\|\beta_k - \beta_k^*\|^2} - \sum_{k=1}^M \frac{\|\eta_k^*\| (\beta_k^T \beta_k^* - 1)}{\|\beta_k - \beta_k^*\|^2} \right) (\tilde{\phi}^2(t) + \tilde{f}^2) \\ &\quad + \xi^T (\phi(p(t)) + f(t)) \\ &\leq -\sum_{k=1}^M \frac{\|\eta_k\|}{2} (\tilde{\phi}^2(t) + \tilde{f}^2) + \xi^T (\phi(p(t)) + f(t)) \\ &\leq -\sum_{k=1}^M \frac{\|\eta_k\|}{2} (\tilde{\phi}^2(t) + \tilde{f}^2) + \frac{Mc}{2N_f} \sum_{i=N_i+1}^N \|\phi_i(p_i(t))\|^2 \\ &\quad + \frac{N_f}{Mc} \xi^T \xi + \frac{Mc}{2N_f} \sum_{i=N_i+1}^N \|f_i(t)\|^2 \\ &\leq \frac{N_f}{Mc} \xi^T \xi - \sum_{k=1}^M \frac{\|\eta_k\| - c}{2} (\tilde{\phi}^2(t) + \tilde{f}^2) \\ &\leq \frac{N_f}{Mc} \xi^T \xi. \quad (27) \end{aligned}$$

Substituting (27) to (26), it follows from (23) that

$$\begin{aligned} \dot{V} &\leq -\left( \frac{k_f \lambda_{\min}(\mathcal{B}_{ff})}{4N\mathcal{S}_0} - \frac{N_f}{Mc} \right) \xi^T \xi \\ &= -\bar{a}V < 0, \quad (28) \end{aligned}$$

where  $\bar{a}$  denotes the exponential convergence rate which is expressed as

$$\bar{a} = \frac{k_f Mc \lambda_{\min}(\mathcal{B}_{ff}) - 4NN_f\mathcal{S}_0}{4NMc\mathcal{S}_0} > 0.$$

Hence, under the protocol (9), the formation error  $\xi$  will converge to zero exponentially. That is to say, all the agents will converge to the target formation exponentially.  $\square$

## B. Stability analysis in the presence of time delay

It is noticeable that time delay always exists in ITS and it should be considered in the control protocol design. This section focuses on the stability analysis of the proposed protocol (9) in the presence of time delays.

Following the system analysis provided in [48], the dynamics of the nonlinear multi-agent time delay system with time-varying actuator faults can be described as

$$\dot{p}_i(t) = u_i(t) + f_i(t) + \phi_i(p_i(t - \tau_i)), \quad i \in \mathcal{V}_f, \quad (29)$$

where  $\tau_i > 0$  denotes the bounded state time delay in the system for the  $i^{\text{th}}$  agent with the boundary  $\tau$ .

Now, we present the stability analysis of the control law (9) in the heterogeneous nonlinear multi-agent time delay system with actuator faults.

**Theorem 2.** *Consider the nonlinear multi-agent time delay system (29). Under Assumptions 1-5 and the control strategy*

(9), if  $k_f$  satisfies (23), all the agents will converge to the target formation asymptotically.

*Proof.* The compact form of the time delay system (29) under the protocol (9) is written as

$$\dot{p} = - \begin{bmatrix} 0 & 0 \\ 0 & I_{dN_f} \end{bmatrix} \bar{H}^T (k_f \zeta + G(\zeta)(\tilde{\phi}^2(t) + \tilde{f}^2)) + \phi(p(t-\tau)) + f(t), \quad (30)$$

where  $\phi(p(t-\tau)) = [0, \dots, \phi_{N_i+1}^T(p_{N_i+1}(t-\tau_{N_i+1})), \dots, \phi_N^T(p_N(t-\tau_N))]^T$ , and

$$G(\zeta) = \left[ \frac{\zeta_1^T}{\|\zeta_1\|^2}, \dots, \frac{\zeta_M^T}{\|\zeta_M\|^2} \right]^T.$$

We construct the Lyapunov function as

$$V = \frac{1}{2} \xi^T \xi + \frac{Mc}{2N_f} V_\tau \quad (31)$$

where

$$V_\tau = \sum_{i=N_i+1}^N \int_{t-\tau_i}^t \|\phi_i(p_i(\sigma))\|^2 d\sigma$$

it can be implied that

$$\dot{V}_\tau = \sum_{i=N_i+1}^N (\|\phi_i(p_i(t))\|^2 - \|\phi_i(p_i(t-\tau_i))\|^2) \quad (32)$$

Hence, the deviation of  $V$  can be described as

$$\begin{aligned} \dot{V} &= \xi^T \dot{p} + \frac{Mc}{2N_f} \sum_{i=N_i+1}^N (\|\phi_i(p_i(t))\|^2 - \|\phi_i(p_i(t-\tau_i))\|^2) \\ &= -k_f \xi^T \bar{H}^T \zeta + \xi^T \bar{H}^T G(\zeta)(\tilde{\phi}^2(t) + \tilde{f}^2) + \xi^T \phi(p(t-\tau)) \\ &\quad + \xi^T f(t) + \frac{Mc}{2N_f} (\|\phi(p(t))\|^2 - \|\phi(p(t-\tau))\|^2) \\ &\leq -k_f p^T \bar{H}^T \zeta + \Pi_1 + \Pi_2 \\ &\leq -k_f \frac{\xi^T \xi \lambda_{\min}(\mathcal{B}_{ff})}{4N\mathcal{S}_0} + \Pi_1 + \Pi_2, \end{aligned} \quad (33)$$

where

$$\Pi_1 = -\xi^T (\bar{H}^T G(\zeta) \tilde{f}^2 - f(t)),$$

and

$$\begin{aligned} \Pi_2 &= -\xi^T (\bar{H}^T G(\zeta) \tilde{\phi}^2(t) - \phi(p(t-\tau))) + \\ &\quad \frac{Mc}{2N_f} (\|\phi(p(t))\|^2 - \|\phi(p(t-\tau))\|^2). \end{aligned}$$

Similar to the discussion in (27), we can get

$$\begin{aligned} \Pi_1 &= -(\eta - \eta^*)^T G(\zeta) \tilde{f}^2 + \xi^T f(t) \\ &\leq -\sum_{k=1}^M \frac{\|\eta_k\|}{2} \tilde{f}^2 + \xi^T f(t) \\ &\leq \frac{N_f}{2Mc} \xi^T \xi - \sum_{k=1}^M \frac{\|\eta_k\| - c}{2} \tilde{f}^2 \leq \frac{N_f}{2Mc} \xi^T \xi, \end{aligned} \quad (34)$$

and

$$\begin{aligned} \Pi_2 &= -(\eta - \eta^*)^T G(\zeta) \tilde{\phi}^2(t) + \xi^T \phi(p(t-\tau)) + \frac{Mc}{2N_f} \\ &\quad (\|\phi(p(t))\|^2 - \|\phi(p(t-\tau))\|^2) \\ &\leq -\sum_{k=1}^M \frac{\|\eta_k\|}{2} \tilde{\phi}^2(t) + \frac{Mc}{2N_f} \|\phi(p(t))\|^2 + \xi^T \phi(p(t-\tau)) \\ &\quad - \frac{Mc}{2N_f} \|\phi(p(t-\tau))\|^2 \\ &\leq \xi^T \phi(p(t-\tau)) - \frac{Mc}{2N_f} \|\phi(p(t-\tau))\|^2 + \tilde{\phi}^2(t) * \\ &\quad \sum_{k=1}^M \frac{c - \|\eta_k\|}{2} \\ &\leq \xi^T \phi(p(t-\tau)) - \frac{Mc}{2N_f} \|\phi(p(t-\tau))\|^2 \\ &\leq \frac{N_f}{2Mc} \xi^T \xi + \frac{Mc}{2N_f} \|\phi(p(t-\tau))\|^2 - \frac{Mc}{2N_f} \|\phi(p(t-\tau))\|^2 \\ &= \frac{N_f}{2Mc} \xi^T \xi. \end{aligned} \quad (35)$$

Substituting (34) and (35) to (33), from (23), it can be obtained that

$$\begin{aligned} \dot{V} &\leq -\frac{k_f Mc \lambda_{\min}(\mathcal{B}_{ff}) - 4NN_f \mathcal{S}_0}{4NMc\mathcal{S}_0} \xi^T \xi \\ &< 0, \end{aligned} \quad (36)$$

Then it follows that, under the protocol (9), the formation error  $\xi$  converges to zero asymptotically. In another word, all the agents will converge to the target formation asymptotically.  $\square$

The fault-tolerant bearing-only formation algorithm is presented in Algorithm 1.

#### IV. FAULT-TOLERANT BEARING FORMATION PROTOCOLS WITH COLLISION-AVOIDANCE

Noting that Theorem 1 and 2 are based on the assumption of collision-free among the agents. In this section, we reconstruct the formation protocol and provide a sufficient condition of collision avoidance to remove Assumptions 4 and 5 as shown in the previous sections. Furthermore, we then improve the collision-free controller with continuous action.

##### A. Collision-avoidance controller design

The collision-free bearing-only formation protocol for the  $i^{\text{th}}$  agent is designed as

$$u_i(t) = \sum_{j \in \mathcal{N}_i} \zeta_{ij} + \Gamma \sum_{j \in \mathcal{N}_i} \bar{\Phi}_i(\zeta_{ij}), \quad i \in \mathcal{V}_f, \quad (37)$$

where  $\Gamma$  is the positive control gain which will be designed later, and the compensation function is modified as

$$\bar{\Phi}_i(\zeta_{ij}) = \begin{cases} Q(t) \frac{\zeta_{ij}}{\|\zeta_{ij}\|}, & \text{when } \|\zeta_{ij}\| \neq 0 \\ 0, & \text{when } \|\zeta_{ij}\| = 0. \end{cases}$$

where

$$Q(t) = \tilde{\phi}(t) + \tilde{f}. \quad (38)$$

**Algorithm 1** Fault-tolerant bearing-only protocol design

- 1: Select  $N_l$  leader agents labeled with  $\{1, 2, \dots, N_l\}$  and  $N_f$  follower agents labeled with  $\{N_l+1, \dots, N\}$ ;
- 2: Set the target formation configuration  $p^*$  and compute the target bearing  $\beta^*$ ;
- 3: Set the initial state for each agent;
- 4: **if** Assumptions 1 and 2 are satisfied **then**
- 5:     Set  $R(t) = \bar{\phi}^2(t) + \bar{f}^2$ ;
- 6:     **if** Assumption 4 is satisfied **then**
- 7:         Set the bidirectional communication graph and the oriented graph among each agent;
- 8:         Compute the edge and bearing vectors for each agent, marked with  $\{1, 2, \dots, M\}$ ;
- 9:         Compute the bearing Laplacian matrix  $\mathcal{B}$ ;
- 10:        **if**  $\mathcal{B}_{ff} > 0$  **then**
- 11:           for the  $k^{th}$  bearing vector
- 12:           **if**  $\|\zeta_k\| \neq 0$  **then**;
- 13:              $\Phi_i(\zeta_k) = R(t) \frac{\zeta_k}{\|\zeta_k\|^2}$ ;
- 14:           **else**
- 15:              $\Phi_i(\zeta_k) = 0$ ;
- 16:           **end if**
- 17:           Set the control gain  $k_f$
- 18:           **if**  $k_f$  satisfies (23) **then**
- 19:             Construct the control law  $u_i$  given in (9);
- 20:           **else**
- 21:             Back to step 17;
- 22:           **end if**
- 23:           **else**
- 24:             Back to step 7;
- 25:           **end if**
- 26:        **else**
- 27:           Back to step 3;
- 28:        **end if**
- 29:     **else**
- 30:         Back to step 1;
- 31:     **end if**

Now, we would like to present the following theorem

**Theorem 3.** Consider the heterogeneous nonlinear leader-follower multi-UAV systems (6). Under Assumptions 1-3 and the control strategy (37). Denote  $\kappa = \min_{i,j \in \mathcal{V}} \|p_i^* - p_j^*\|$ , if the initial state of each agent satisfies

$$\|\xi(0)\| \leq \frac{\kappa - c}{\sqrt{N_f}}, \quad (39)$$

there is no collision between each agent during the formation. Furthermore, all the agents will converge to the target formation exponentially by selecting the control gain

$$\Gamma \geq 2\sqrt{\frac{N_f}{\lambda_{\min}(\mathcal{B}_{ff})}}. \quad (40)$$

*Proof.* The compact form of (6) by implementing the collision-avoidance protocol (37) is expressed as

$$\dot{p} = - \begin{bmatrix} 0 & 0 \\ 0 & I_{dN_f} \end{bmatrix} \bar{H}^T (\zeta + \Gamma \bar{\Phi}(\zeta)) + \phi(p(t)) + f(t), \quad (41)$$

where

$$\bar{\Phi}(\zeta) = Q(t) \begin{bmatrix} \frac{\zeta_1^T}{\|\zeta_1\|}, \dots, \frac{\zeta_M^T}{\|\zeta_M\|} \end{bmatrix}^T.$$

Choosing the Lyapunov candidate as

$$V = \frac{1}{2} \xi^T \xi. \quad (42)$$

The deviation of  $V$  is computed as

$$\begin{aligned} \dot{V} &= \xi^T \dot{p} \\ &= -\xi^T \bar{H}^T \zeta - \Gamma \xi^T \bar{H}^T \bar{\Phi}(\zeta) + \xi^T (\phi(p(t)) + f(t)) \\ &\leq -p^T \bar{H}^T \zeta - \Gamma \xi^T \bar{H}^T \bar{\Phi}(\zeta) + \xi^T (\phi(p(t)) + f(t)) \\ &= -p^T \bar{H}^T \zeta + \Pi_3 + \Pi_4, \end{aligned} \quad (43)$$

where

$$\Pi_3 = -\Gamma \xi^T \bar{H}^T \bar{\Phi}(\zeta), \quad \Pi_4 = \xi^T (\phi(p(t)) + f(t)).$$

It can be obtained from the definition of  $\bar{\Phi}$  that

$$\begin{aligned} \Pi_3 &= -(\eta - \eta^*)^T \bar{\Phi}(\zeta) \\ &= -\Gamma \left( \sum_{k=1}^M \frac{\eta_k^T \beta_k - \eta_k^T \beta_k^*}{\|\beta_k - \beta_k^*\|} - \sum_{k=1}^M \frac{\eta_k^{*T} \beta_k - \eta_k^{*T} \beta_k^*}{\|\beta_k - \beta_k^*\|} \right) Q(t) \\ &= -\Gamma \left( \sum_{k=1}^M \frac{\|\eta_k\| (1 - \beta_k^T \beta_k^*)}{\|\beta_k - \beta_k^*\|} - \sum_{k=1}^M \frac{\|\eta_k^*\| (\beta_k^T \beta_k^* - 1)}{\|\beta_k - \beta_k^*\|} \right) Q(t) \\ &\leq -\frac{\Gamma}{2} \sum_{k=1}^M \|\eta_k\| \|\zeta_k\| Q(t) \\ &\leq -\sqrt{\frac{N_f}{\lambda_{\min}(\mathcal{B}_{ff})}} \sum_{k=1}^M \|\eta_k\| \|\zeta_k\| Q(t) \end{aligned} \quad (44)$$

From (22), we have

$$\begin{aligned} \|\xi\| &\leq \sqrt{\frac{1}{\lambda_{\min}(\mathcal{B}_{ff})} \sum_{k=1}^M \|\eta_k\|^2 \|\zeta_k\|^2} \\ &\leq \sqrt{\frac{1}{\lambda_{\min}(\mathcal{B}_{ff})} \sum_{k=1}^M \|\eta_k\| \|\zeta_k\|}. \end{aligned} \quad (45)$$

Hence, it follows that

$$\begin{aligned} \Pi_4 &\leq \|\xi\| \|\phi(p(t)) + f(t)\| \\ &\leq \|\xi\| (\|\phi(p(t))\| + \|f(t)\|) \\ &\leq \sqrt{\frac{N_f}{\lambda_{\min}(\mathcal{B}_{ff})}} \sum_{k=1}^M \|\eta_k\| \|\zeta_k\| Q(t). \end{aligned} \quad (46)$$

Combining (43), (44), and (46), from Lemma 2 and (22), we can get

$$\begin{aligned} \dot{V} &\leq -p^T \bar{H}^T \zeta + \Pi_3 + \Pi_4 \\ &\leq -p^T \bar{H}^T \zeta \\ &\leq -\frac{\lambda_{\min}(\mathcal{B}_{ff})}{2 \max_k \|\eta_k\|} \xi^T \xi \\ &\leq 0. \end{aligned} \quad (47)$$

In another words,  $\xi(t) \leq \xi(0)$  for any  $t > 0$ . According to

(39), we can observe that

$$\begin{aligned}
\|\eta_k(t)\| &= \|\eta_{ij}(t)\| = \|(p_i^* - p_j^*) + (p_i - p_i^*) - (p_j - p_j^*)\| \\
&\geq \|\eta_k^*\| - \|\xi_i(t)\| - \|\xi_j(t)\| \\
&\geq \|\eta_k^*\| - \sum_{i=1}^N \|\xi_i(t)\| \\
&\geq \|\eta_k^*\| - \sqrt{N_f} \|\xi(t)\| \\
&\geq \|\eta_k^*\| - \sqrt{N_f} \|\xi(0)\| \\
&\geq \|\eta_k^*\| - \kappa + c \geq c.
\end{aligned} \tag{48}$$

Hence, there is no collision between each agent during the formation task under the condition (39).

Noting that

$$\begin{aligned}
\max_k \|\eta_k\| &\leq \|\eta\| \\
&\leq \|\bar{H}\| \|p - p^* + p^*\| \\
&\leq \|\bar{H}\| (\|\xi(t)\| + \|p^*\|) \\
&\leq \|\bar{H}\| (\|\xi(0)\| + \|p^*\|),
\end{aligned} \tag{49}$$

Together with (47), we have

$$\dot{V} \leq -\frac{\lambda_{\min}(\mathcal{B}_{ff})}{2\|\bar{H}\|(\|\xi(0)\| + \|p^*\|)} \xi^T \xi = -\tilde{a}V. \tag{50}$$

where  $\tilde{a}$  stands for the exponential converge rate which is denoted as

$$\tilde{a} = \frac{\lambda_{\min}(\mathcal{B}_{ff})}{\|\bar{H}\|(\|\xi(0)\| + \|p^*\|)} > 0.$$

That is to say, the formation error converges to zero exponentially.  $\square$

### B. Collision-avoidance protocol design with continuous action

It can be observed that the collision-avoidance protocol (37) is discontinuous. This drawback is possible to trigger the chattering effect in the control signal in real implementation [49]. According to [50], the boundary layer technique can be utilized to minimize this restriction. Enlightened by this method, the continuous collision-avoidance protocol is designed as

$$u_i(t) = \sum_{j \in \mathcal{N}_i} \zeta_{ij} + \Gamma \sum_{j \in \mathcal{N}_i} \bar{\Phi}_c(\zeta_{ij}), \quad i \in \mathcal{V}_f, \tag{51}$$

with the compensation function  $\bar{\Phi}_c$  is modified as

$$\bar{\Phi}_c(\zeta_{ij}) = \begin{cases} Q(t) \frac{\zeta_{ij}}{\|\zeta_{ij}\|}, & \text{when } \|\zeta_{ij}\| > \varepsilon \\ Q(t) \frac{\zeta_{ij}}{\varepsilon}, & \text{when } \|\zeta_{ij}\| \leq \varepsilon. \end{cases} \tag{52}$$

The following theorem reveals the stability of the collision-avoidance protocol with continuous form.

**Theorem 4.** *Consider the heterogeneous nonlinear leader-follower multi-UAV systems (6). Under Assumption 1-3 and the control strategy (51). Suppose  $\dot{\phi}(t) \leq \phi^*$ . There is no collision between each agent during the formation if (39) holds. Furthermore, the formation error  $\xi$  of the agents will*

converge to a bounded set

$$\Omega = \left\{ \xi : \|\xi\| \leq \frac{\psi(\varepsilon)}{1 - \psi(\varepsilon)} \|p^*\| \right\}.$$

if the control gain  $\Gamma$  satisfies (40), and  $\varepsilon$  is small enough such that  $\psi(\varepsilon)$  is small enough, where

$$\psi(\varepsilon) = \sqrt[4]{\frac{\varepsilon^2 Q^2 M^2 N_f}{\lambda_{\min}^3(\mathcal{B}_{ff})} \|\bar{H}\|},$$

and  $Q = \phi^* + \tilde{f}$ .

*Proof.* The compact form of (6) under the modified protocol (51) is described as

$$\dot{p} = - \begin{bmatrix} 0 & 0 \\ 0 & I_{dN_f} \end{bmatrix} \bar{H}^T (\zeta + \Gamma \bar{\Phi}_c(\zeta)) + \phi(p(t)) + f(t), \tag{53}$$

where

$$\bar{\Phi}_c(\zeta) = [\bar{\phi}_c^T(\zeta_1), \dots, \bar{\phi}_c^T(\zeta_M)]^T.$$

Considering the Lyapunov function as

$$V = \frac{1}{2} \xi^T \xi. \tag{54}$$

It can be obtained from (43) that

$$\begin{aligned}
\dot{V} &= \xi^T \dot{p} \\
&\leq -p^T \bar{H}^T \zeta + \Pi_3^c + \Pi_4,
\end{aligned} \tag{55}$$

where

$$\Pi_3^c = -\Gamma \xi^T \bar{H}^T \bar{\Phi}_c(\zeta), \quad \Pi_4 = \xi^T (\phi(p(t)) + f(t)).$$

To analyse the modified compensation function  $\bar{\Phi}_c$ . Three cases should be discussed in the following stage.

*Case 1:* if  $\|\xi_k\| > \varepsilon, \forall k \in \{1, 2, \dots, M\}$ . From (44), we can get

$$\Pi_3^c = \Pi_3 \leq -\sqrt{\frac{N_f}{\lambda_{\min}(\mathcal{B}_{ff})}} \sum_{k=1}^M \|\eta_k\| \|\zeta_k\| Q(t). \tag{56}$$

Based on (46), we have

$$\Pi_3^c + \Pi_4 \leq 0. \tag{57}$$

*Case 2:* if  $\|\xi_k\| \leq \varepsilon, \forall k \in \{1, 2, \dots, M\}$ . In one hand

$$\begin{aligned}
\Pi_3^c &= -(\eta - \eta^*)^T \bar{\Phi}_c(\zeta) \\
&= -\Gamma \left( \sum_{k=1}^M \frac{\eta_k^T \beta_k - \eta_k^T \beta_k^*}{\varepsilon} - \sum_{k=1}^M \frac{\eta_k^{*T} \beta_k - \eta_k^{*T} \beta_k^*}{\varepsilon} \right) Q(t) \\
&= -\Gamma \left( \sum_{k=1}^M \frac{\|\eta_k\| (1 - \beta_k^T \beta_k^*)}{\varepsilon} - \sum_{k=1}^M \frac{\|\eta_k^*\| (\beta_k^T \beta_k^* - 1)}{\varepsilon} \right) Q(t) \\
&\leq -\frac{\Gamma}{2} \sum_{k=1}^M \frac{\|\eta_k\| \|\zeta_k\|^2}{\varepsilon} Q(t) \\
&\leq 0.
\end{aligned} \tag{58}$$

In another hand, from (46) and (52), it follows that

$$\begin{aligned} \Pi_4 &\leq \sqrt{\frac{N_f}{\lambda_{\min}(\mathcal{B}_{ff})}} \sum_{k=1}^M \|\eta_k\| \|\zeta_k\| Q(t). \\ &\leq \varepsilon \sqrt{\frac{M^2 N_f}{\lambda_{\min}(\mathcal{B}_{ff})}} \|\eta\| Q \end{aligned} \quad (59)$$

Hence, we have

$$\Pi_3^c + \Pi_4 \leq \varepsilon \sqrt{\frac{M^2 N_f}{\lambda_{\min}(\mathcal{B}_{ff})}} \|\eta\| Q. \quad (60)$$

*Case 3:* if  $\|\xi_k\|$  does not satisfy Case 1 or Case 2. In another word, we can supposed that  $\|\xi_k\| > \varepsilon, \forall k \in \{1, 2, \dots, M_1\}$ , and  $\|\xi_k\| \leq \varepsilon, \forall k \in \{M_1, \dots, M\}$ . According to (44) and (58), it can be observed that

$$\begin{aligned} \Pi_3^c &= -(\eta - \eta^*)^T \bar{\Phi}_c(\zeta) \\ &= -\Gamma \left( \sum_{k=1}^{M_1} \frac{\eta_k^T \beta_k - \eta_k^T \beta_k^*}{\|\beta_k - \beta_k^*\|} - \sum_{k=1}^{M_1} \frac{\eta_k^{*T} \beta_k - \eta_k^{*T} \beta_k^*}{\|\beta_k - \beta_k^*\|} \right) Q(t) \\ &\quad - \Gamma \left( \sum_{k=M_1+1}^M \frac{\eta_k^T \beta_k - \eta_k^T \beta_k^*}{\varepsilon} - \sum_{k=M_1+1}^M \frac{\eta_k^{*T} \beta_k - \eta_k^{*T} \beta_k^*}{\varepsilon} \right) Q(t) \\ &= -\Gamma \left( \sum_{k=1}^{M_1} \frac{\|\eta_k\| (1 - \beta_k^T \beta_k^*)}{\|\beta_k - \beta_k^*\|} - \sum_{k=1}^{M_1} \frac{\|\eta_k^*\| (\beta_k^T \beta_k^* - 1)}{\|\beta_k - \beta_k^*\|} \right) Q(t) \\ &\quad - \Gamma \left( \sum_{k=M_1+1}^M \frac{\|\eta_k\| (1 - \beta_k^T \beta_k^*)}{\varepsilon} - \sum_{k=M_1+1}^M \frac{\|\eta_k^*\| (\beta_k^T \beta_k^* - 1)}{\varepsilon} \right) Q(t) \\ &\leq -\frac{\Gamma}{2} \sum_{k=1}^{M_1} \|\eta_k\| \|\zeta_k\| Q(t) \\ &\leq -\sqrt{\frac{N_f}{\lambda_{\min}(\mathcal{B}_{ff})}} \sum_{k=1}^{M_1} \|\eta_k\| \|\zeta_k\| Q(t), \end{aligned} \quad (61)$$

and

$$\begin{aligned} \Pi_4 &\leq \sqrt{\frac{N_f}{\lambda_{\min}(\mathcal{B}_{ff})}} \sum_{k=1}^M \|\eta_k\| \|\zeta_k\| Q(t) \\ &\leq \sqrt{\frac{N_f}{\lambda_{\min}(\mathcal{B}_{ff})}} \sum_{k=1}^{M_1} \|\eta_k\| \|\zeta_k\| Q(t) + \\ &\quad \varepsilon \sqrt{\frac{(M - M_1)^2 N_f}{\lambda_{\min}(\mathcal{B}_{ff})}} \|\eta\| Q \end{aligned} \quad (62)$$

Then, it follows that

$$\Pi_3^c + \Pi_4 \leq \varepsilon \sqrt{\frac{(M - M_1)^2 N_f}{\lambda_{\min}(\mathcal{B}_{ff})}} \|\eta\| Q. \quad (63)$$

Based on the above discussion, it can be implied that  $\Pi_3^c + \Pi_4$  satisfies (60) for all the cases. Hence, we can substitute (60)

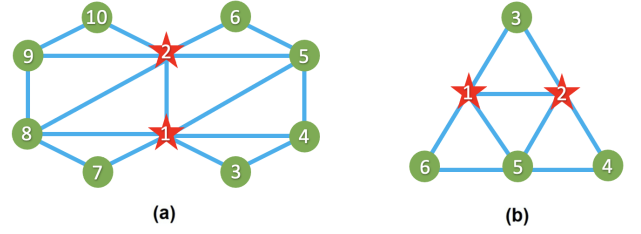


Fig. 3. The communications between each agent (a) Case 1 and 2; (b) Case 3.

to (55), it follows by

$$\begin{aligned} \dot{V} &\leq -p^T \bar{H}^T \zeta + \Pi_3^c + \Pi_4 \\ &\leq -\frac{\lambda_{\min}(\mathcal{B}_{ff})}{2\|\eta\|} \xi^T \xi + \varepsilon \sqrt{\frac{M^2 N_f}{\lambda_{\min}(\mathcal{B}_{ff})}} \|\eta\| Q \\ &\leq -\frac{\lambda_{\min}(\mathcal{B}_{ff})}{2\|\bar{H}\|(\|\xi\| + \|p^*\|)} \xi^T \xi + \varepsilon \sqrt{\frac{M^2 N_f}{\lambda_{\min}(\mathcal{B}_{ff})}} \|\bar{H}\|(\|\xi\| \\ &\quad + \|p^*\|) Q = h(\xi). \end{aligned} \quad (64)$$

Solving the inequality  $h(\xi) < 0$ , we have

$$\|\xi(t)\| > \frac{\psi(\varepsilon)}{1 - \psi(\varepsilon)} \|p^*\|. \quad (65)$$

Define the bounded set  $\Omega$  as

$$\Omega = \left\{ \xi : \|\xi\| \leq \frac{\psi(\varepsilon)}{1 - \psi(\varepsilon)} \|p^*\| \right\}.$$

Denote  $\bar{\Omega}$  as supplementary set of  $\Omega$ . If  $\xi \in \bar{\Omega}$ , it can be obtained that

$$\dot{V} \leq 0. \quad (66)$$

That is to say, the formation error  $\xi$  of the agents will converge to a bounded set  $\Omega$  by implementing the protocol (51), and there is no collision between each agent during the process under the condition (39). This completes the proof.  $\square$

The collision-free fault-tolerant bearing-only formation algorithm is presented in Algorithm 2.

## V. SIMULATION RESULTS

In this section, four case studies are provided to validate the effectiveness of the proposed theoretical results.

### A. Case 1: Fault-tolerant bearing-only formation tracking

The first case study focuses on the effectiveness of the proposed fault-tolerant bearing-only formation protocol (9). Considering the multi-UAV networks with two stationary leaders and eight followers. The network connections among the agents are demonstrated in Fig. 3(a), where the red stars denote the leaders and the green circles represent the followers. According to the labels in Fig. 3(a), we obtain that  $\mathcal{V}_l = \{1, 2\}$ , and  $\mathcal{V}_f = \{3, 4, 5, 6, 7, 8, 9, 10\}$ . The target formation is defined as two hexagons together in a 3D space. Denoted

---

**Algorithm 2** Collision-free fault-tolerant bearing-only protocol design
 

---

- 1: Select  $N_l$  leader agents labeled with  $\{1, 2, \dots, N_l\}$  and  $N_f$  follower agents labeled with  $\{N_l+1, \dots, N\}$ ;
  - 2: Set the target formation configuration  $p^*$  and compute the target bearing  $\beta^*$ ;
  - 3: Set the initial state for each agent;
  - 4: **if** Collision-free condition (39) does not hold **then**
  - 5: Back to step 3;
  - 6: **end if**
  - 7: **if** Assumptions 1 and 2 are satisfied **then**
  - 8: Set  $Q(t) = \tilde{\phi}(t) + \tilde{f}$ ;
  - 9: Set the bidirectional communication graph and the oriented graph among each agent;
  - 10: Compute the edge and bearing vectors for each agent, marked with  $\{1, 2, \dots, M\}$ ;
  - 11: Compute the bearing Laplacian matrix  $\mathcal{B}$ ;
  - 12: **if**  $\mathcal{B}_{ff} > 0$  **then**
  - 13: Set a threshold  $\varepsilon$ , for the  $k^{th}$  bearing vector;
  - 14: **if**  $\|\zeta_k\| > \varepsilon$  **then**
  - 15:  $\bar{\Phi}_c(\zeta_k) = Q(t) \frac{\zeta_k}{\|\zeta_k\|}$ ;
  - 16: **else**
  - 17:  $\bar{\Phi}_c(\zeta_k) = Q(t) \frac{\zeta_k}{\varepsilon}$ ;
  - 18: **end if**
  - 19: Set the control gain  $\Gamma$
  - 20: **if**  $\Gamma$  satisfies (40) **then**
  - 21: Construct the control law  $u_i$  given in (51);
  - 22: **else**
  - 23: Back to step 19;
  - 24: **end if**
  - 25: **else**
  - 26: Back to step 9;
  - 27: **end if**
  - 28: **else**
  - 29: Back to step 1;
  - 30: **end if**
- 

the position of each agent in  $\mathbb{R}^3$  as  $p_i = [p_{ix}, p_{iy}, p_{iz}]^T$ ,  $i \in \mathcal{V}$ . We choose the nonlinear function  $\phi_i$  for the  $i^{th}$  agent as

$$\phi_i = \begin{bmatrix} \frac{\sin(ip_{ix}(t)\pi/10)\sin(t/10)}{3} \\ -\frac{\sin(ip_{iy}(t)\pi/10)\sin(t/10)}{3} \\ \frac{\cos(ip_{iz}(t)\pi/10)\sin(t/10)}{3} \end{bmatrix}, \quad i \in \mathcal{V}_f. \quad (67)$$

The actuator faults are set by

$$f_i = \begin{bmatrix} \frac{\sin(t + \frac{(i-1)\pi}{15})}{3} \\ \frac{\cos(t + \frac{(i-1)\pi}{15})}{3} \\ -\frac{\cos(t + \frac{(i-1)\pi}{15})}{3} \end{bmatrix}, \quad i \in \mathcal{V}_f. \quad (68)$$

It can be implied that  $\|\phi_i\| \leq \sin(t/10)$ , and  $\|f_i\| \leq 1$ . Consequently, the term  $R(t)$  in controller (9) can be selected as

$$R(t) = 1 + \sin^2 \frac{t}{10}. \quad (69)$$

The leaders are fixed at  $(2, 1, 6)$  and  $(4, 1, 6)$ , and the initial positions of the followers are set as  $(5, 1, 1)$ ,  $(4, 2, 0)$ ,  $(3, 2, 8)$ ,

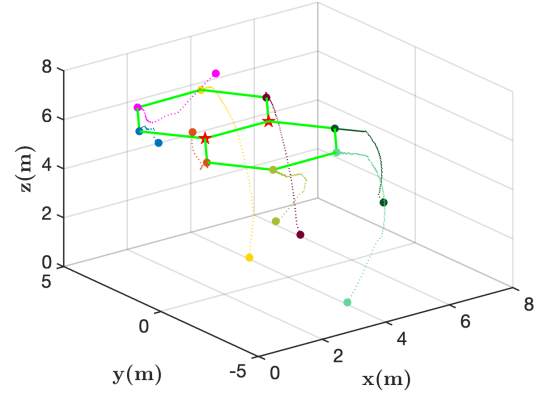


Fig. 4. The trajectory of each follower agent in case 1.

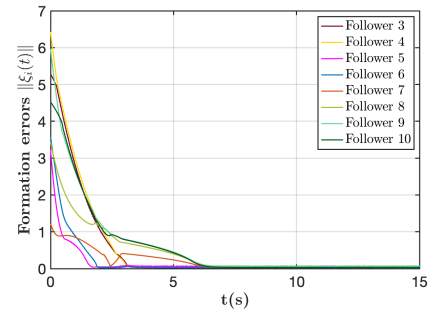


Fig. 5. The formation error of each follower agent in case 1.

$(3, 5, 4)$ ,  $(1, 0, 7)$ ,  $(3, -1, 3)$ ,  $(4, -3, 0)$ , and  $(7, 0, 2)$ . We further adjust the control gain as  $k_f = 20$  to satisfy the condition in Theorem 1.

Fig. 4 illustrates the trajectory of each follower during the formation by applying the protocol (9). The states of the leaders are labeled by two red stars, and the movements of the followers are denoted by eight dashed lines with different colors. The time variation of the formation error  $\|\xi_i(t)\|$  for each follower is elucidated in Fig. 5. The formation errors converge to zero and all the follower agents will converge to the target formation. Therefore, it can be obtained the formation task can be accomplished by the proposed controller (9).

### B. Case 2: Formation tracking in the presence of various time delays

In this case, time delays in system dynamics are taken into consideration to verify the robustness of the proposed bearing-only formation protocol (9). The setup of the agents is the same as that in Case 1. Specially, the nonlinear function  $\phi_i$  with time delays for the  $i^{th}$  follower agent is reset as

$$\phi_i(p_i(t-\tau)) = \begin{bmatrix} \frac{\sin(ip_{ix}(t-\tau)\pi/2)}{3} \\ -\frac{\sin(ip_{iy}(t-\tau)\pi/2)}{3} \\ \frac{\cos(ip_{iz}(t-\tau)\pi/2)}{3} \end{bmatrix}, \quad i \in \mathcal{V}_f. \quad (70)$$

The actuator faults are expressed by equation (68). It can be computed that  $\|\phi_i\| \leq 1$ , and  $\|f_i\| \leq 1$ . Therefore, we can choose  $R(t) = 2$  in this case.

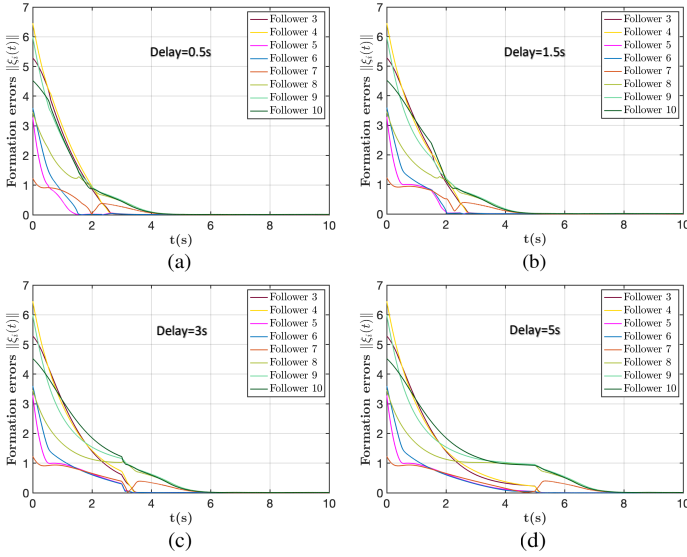


Fig. 6. The formation error of each follower agent in the presence of time delays with (a)  $\tau_1 = 0.5$  s, (b)  $\tau_2 = 1.5$  s, (c)  $\tau_3 = 3$  s, and (d)  $\tau_4 = 5$  s.

We test four examples with different time delays set as  $\tau_1 = 0.5$  s,  $\tau_2 = 1.5$  s,  $\tau_3 = 3$  s, and  $\tau_4 = 5$  s. By implementing Algorithm 1 to each follower, the time variations of the formation error  $\|\xi_i(t)\|$  for each follower are displayed in Fig. 6(a)-(d). It can be observed that all formation errors will converge to zero with various time delays. That is to say, the proposed protocol (9) is robust if there exist certain time delays in the system dynamics.

### C. Case 3: Formation tracking protocol with continuous action

The case study on the continuous bearing-only protocol (51) is shown in this section. The drones are set with the same altitudes. Hence, the dimension can be degraded from 3D to 2D space. We aim to utilize two leader agents fixed at [9, 9] and [9, 3], and four follower agents as the multi-UAV networks to form four equilateral triangles together. The interaction topology between each agent is shown in Fig. 3(b). It can be obtained that  $\mathcal{V}_l = \{1, 2\}$ , and  $\mathcal{V}_f = \{3, 4, 5, 6\}$  from the labels in Fig. 3(b). The initial positions of the followers are shown in Fig. 7(a). Denote the state of each agent in  $\mathbb{R}^2$  as  $p_i = [p_{ix}, p_{iy}]^T$ , the nonlinear function  $\phi_i$  of the  $i^{th}$  agent is defined as

$$\phi_i = \begin{bmatrix} \frac{t \sin(ip_{ix}(t)\pi/8)}{3(t+1)} \\ \frac{t \cos(ip_{iy}(t)\pi/8)}{3(t+1)} \end{bmatrix}, \quad i \in \mathcal{V}_f. \quad (71)$$

The actuator faults are described as

$$f_i = \begin{bmatrix} \frac{(t+2)\cos(t + \frac{(i-1)\pi}{15})}{6(t+1)} \\ \frac{(t+2)\sin(t + \frac{(i-1)\pi}{15})}{6(t+1)} \end{bmatrix}, \quad i \in \mathcal{V}_f. \quad (72)$$

It can be obtained that  $\|\phi_i\| \leq t/(t+1) \leq 1$ , and  $\|f_i\| \leq 1$ . Hence, we can set  $Q(t) = 1 + t/(t+1)$  and  $Q = 2$ .

According to Algorithm 2, we set the threshold as  $\varepsilon = 10^{-3}$ . The control gain can be selected as  $\Gamma = 10$ . The trajectories of the follower agents are reflected in Fig. 7 at different time

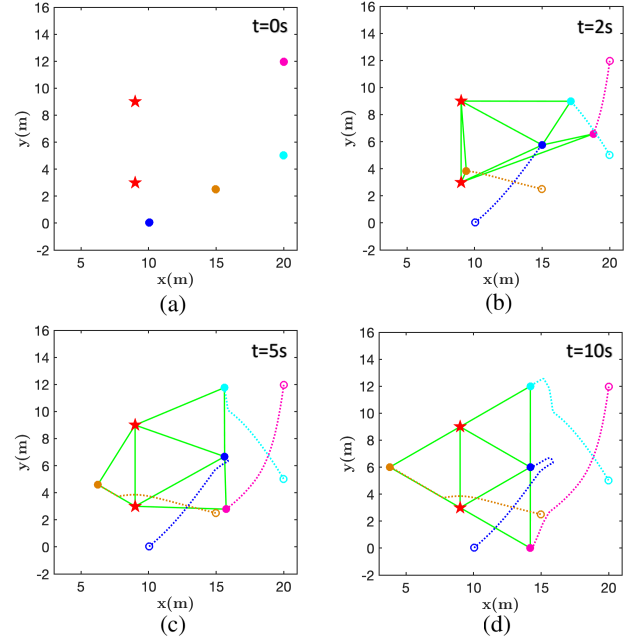


Fig. 7. The trajectories of the follower agents at time (a)  $t = 0$ s, (b)  $t = 2$ s, (c)  $t = 5$ s, and (d)  $t = 10$ s in case 3.

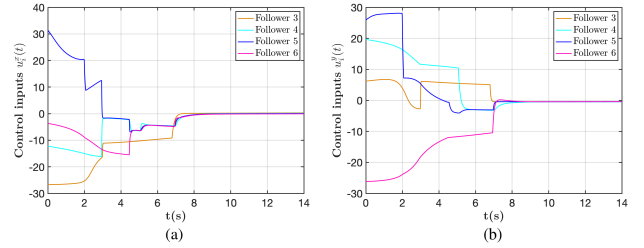


Fig. 8. The control inputs of each follower agent along (a) x-axis, and (b) y-axis in case 3.

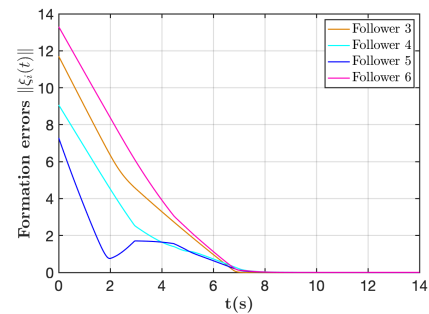


Fig. 9. The formation error of each follower agent in case 3.

instants. It can be verified that all the followers converge to the target formation within 10 s. From the snapshots of the positions of the agents, it can also be easily seen that there is no collision among the agents during the formation tracking task. Fig. 8 reveals that the control inputs  $u_i$  along the x-axis and y-axis are continuous and will converge to zero. Fig. 9 also demonstrates that formation error  $\|\xi_i\|$  of each follower will converge to a small bounded set if the positive threshold  $\varepsilon$  is

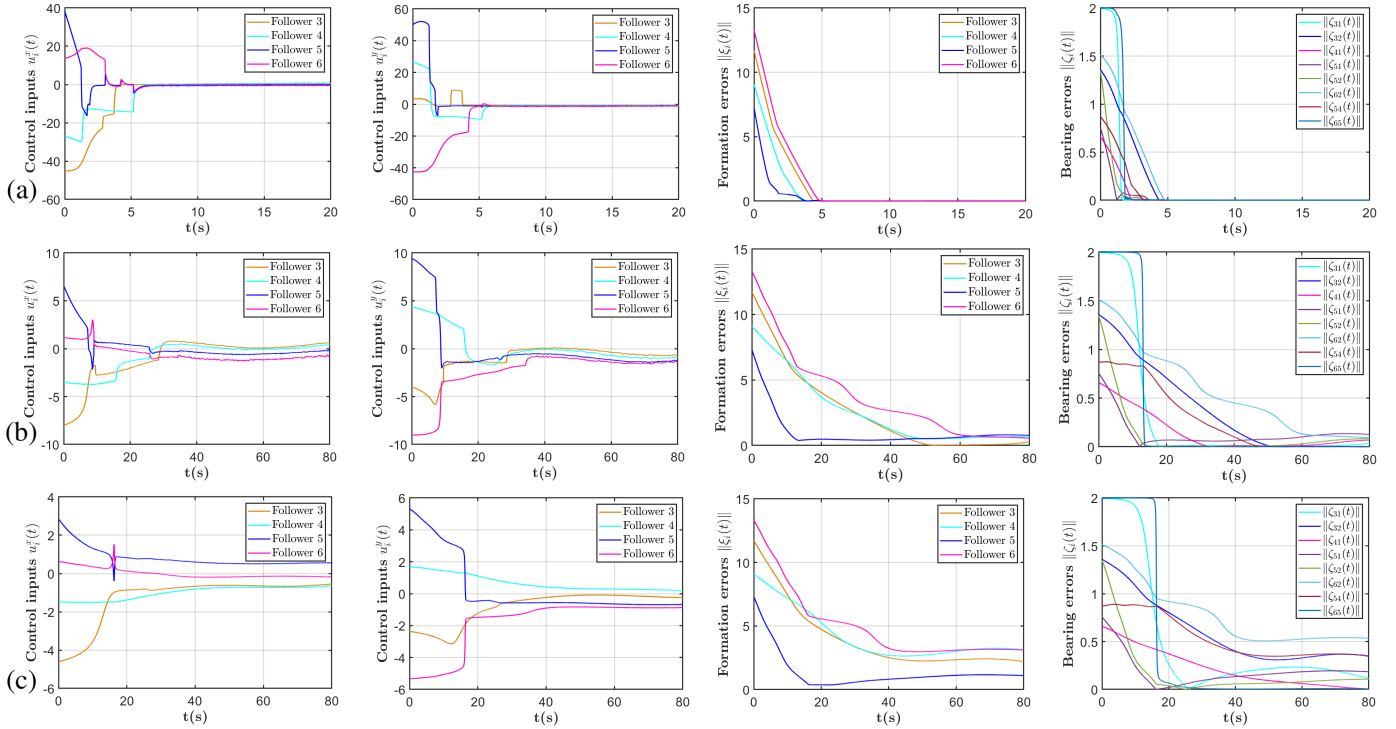


Fig. 10. Simulation results illustrate the performance of the bearing-only protocol with different parameters (a)  $\Gamma = 12$ , (b)  $\Gamma = 2$ , and (c)  $\Gamma = 0.01$ .

small enough. This validates the feasibility of the fault-tolerant bearing-only formation protocol (51).

In order to explore the effect of the heterogeneous nonlinear items in the systems, we further design the simulations to demonstrate the performance of the proposed protocol with different parameters. The set up in this simulation is same as set in this section. The actuator faults are generated by (72). The heterogeneous nonlinear function of the  $i^{th}$  UAV is described as

$$\phi_i = i \begin{bmatrix} \frac{t \sin(ip_{ix}(t)\pi/8)}{6(t+1)} \\ \frac{t \cos(ip_{iy}(t)\pi/8)}{6(t+1)} \end{bmatrix}, i \in \mathcal{V}_f. \quad (73)$$

Similarly, we can also choose  $Q = 2$  and  $\varepsilon = 10^{-3}$ . By implementing the proposed algorithm (51) with (a)  $\Gamma = 12$ , (b)  $\Gamma = 2$ , and (c)  $\Gamma = 0.01$ , the results are shown in Fig. 10. We can obtain from Fig. 10 (c) that the heterogeneous nonlinear items are hardly to be diminished if the parameter  $\Gamma$  is too small ( $\Gamma = 0.01$ ). After increasing the value of  $\Gamma$  equals to 2, it can be observed from Fig. 10 (b) that the heterogeneous nonlinear items can be partly tackled by the compensation function and the formation and bearing errors are closer to zero. Moreover, if we select the parameter  $\Gamma$  satisfies the condition in Theorem 4. According to Fig. 10 (a), the heterogeneous nonlinear items can be eliminated by the controller (51). That is to say, the effect of the heterogeneous nonlinear function is related to the parameter  $\Gamma$  which should be designed carefully to satisfy the condition in Theorem 4.

#### D. Comparison with traditional bearing-only formation tracking strategy

In this section, the comparison between the proposed

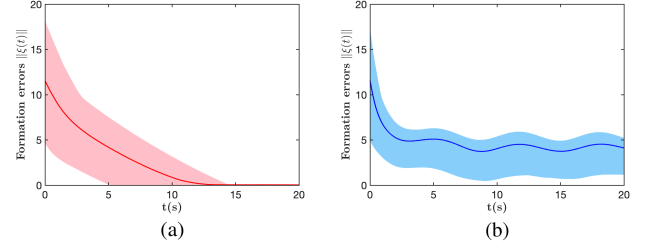


Fig. 11. Performance of (a) proposed algorithm, (b) traditional bearing-only algorithm.

bearing-only strategy with the traditional bearing-only protocol proposed in [47] is explored to further illustrate the novelty of the compensation function. Two fixed leaders and four followers are adopted for both cases with the same target formation as shown in Case 3. The nonlinear function and the actuator faults are generated by (71) and (72). The initial states of the followers are randomly selected from  $[-5, 5] \times [-5, 5]$ . We run 50 times simulation for each protocol and the results are shown in Fig. 11 (a) and (b). The red and blue zones demonstrate the results of the proposed and traditional algorithms, and the blue and red solid lines denote the average results. Since the system is nonlinear and there exist actuator faults in the controller. The formation error cannot converge to zero under the traditional method (Fig. 11(b)). However, these factors will be eliminated if the compensation function is implemented in the controller (Fig. 11(a)). Hence, the proposed protocol shows a better robust performance than the traditional algorithm when dealing with complex agent dynamics, which may be more reliable when implemented in real robotic platforms.

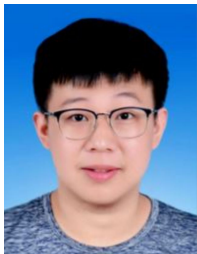
## VI. CONCLUSION

This paper addresses the bearing coordination problem for nonlinear multi-UAV networks with actuator faults. We proposed the fault-tolerant bearing-only formation protocols for each follower in the system. A novel compensation function based only on bearing measurements is designed to deal with nonlinear dynamics and the faults in the system. We further discuss the robustness of the protocol if there exist time delays in the system. Moreover, we present a new scheme for the compensation function and a sufficient condition to guarantee that all the agents are collision-free. The stability of the collision-free algorithm with continuous action can be also ensured by Lyapunov method. Finally, we provide simulations to verify the effectiveness of the proposed protocols. In the future, more characteristics of the UAVs will be addressed in the control systems design to further strengthen the feasibility and real-world coordination performance.

## REFERENCES

- [1] A. V. Savkin and H. Huang, "Navigation of a uav network for optimal surveillance of a group of ground targets moving along a road," *IEEE Transactions on Intelligent Transportation Systems*, vol. 23, no. 7, pp. 9281–9285, 2021.
- [2] F. Rejabi-Bana, J. Hu, T. Krajník, and F. Arvin, "Unified robust path planning and optimal trajectory generation for efficient 3D area coverage of quadrotor UAVs," *IEEE Transactions on Intelligent Transportation Systems*, 2023.
- [3] R. G. Ribeiro, L. P. Cota, T. A. Euzébio, J. A. Ramírez, and F. G. Guimarães, "Unmanned-aerial-vehicle routing problem with mobile charging stations for assisting search and rescue missions in postdisaster scenarios," *IEEE transactions on systems, man, and cybernetics: Systems*, vol. 52, no. 11, pp. 6682–6696, 2021.
- [4] S. Xie, J. Hu, P. Bhowmick, Z. Ding, and F. Arvin, "Distributed motion planning for safe autonomous vehicle overtaking via artificial potential field," *IEEE Transactions on Intelligent Transportation Systems*, vol. 23, no. 11, pp. 21 531–21 547, 2022.
- [5] S. Xie, J. Hu, Z. Ding, and F. Arvin, "Cooperative adaptive cruise control for connected autonomous vehicles using spring damping energy model," *IEEE Transactions on Vehicular Technology*, vol. 72, no. 3, pp. 2974–2987, 2022.
- [6] M. Stefanec, D. N. Hofstadler, T. Krajník, A. E. Turgut, H. Alemdar, B. Lennox, E. Şahin, F. Arvin, and T. Schmicl, "A minimally invasive approach towards "ecosystem hacking" with honeybees," *Frontiers in Robotics and AI*, vol. 9, 2022.
- [7] C. Bai, P. Yan, W. Pan, and J. Guo, "Learning-based multi-robot formation control with obstacle avoidance," *IEEE Transactions on Intelligent Transportation Systems*, vol. 23, no. 8, pp. 11 811–11 822, 2021.
- [8] X. Sun, G. Wang, Y. Fan, D. Mu, and B. Qiu, "A formation autonomous navigation system for unmanned surface vehicles with distributed control strategy," *IEEE Transactions on Intelligent Transportation Systems*, vol. 22, no. 5, pp. 2834–2845, 2020.
- [9] W. Liu, H. Niu, I. Jang, G. Herrmann, and J. Carrasco, "Distributed neural networks training for robotic manipulation with consensus algorithm," *IEEE Transactions on Neural Networks and Learning Systems*, vol. 35, no. 2, pp. 2732–2746, 2024.
- [10] W. Liu, H. Niu, W. Pan, G. Herrmann, and J. Carrasco, "Sim-and-real reinforcement learning for manipulation: A consensus-based approach," *IEEE International Conference on Robotics and Automation (ICRA)*, 2023.
- [11] F. Chen and D. V. Dimarogonas, "Leader–follower formation control with prescribed performance guarantees," *IEEE Transactions on Control of Network Systems*, vol. 8, no. 1, pp. 450–461, 2020.
- [12] K. Wu, J. Hu, B. Lennox, and F. Arvin, "Sdp-based robust formation-containment coordination of swarm robotic systems with input saturation," *Journal of Intelligent & Robotic Systems*, vol. 102, no. 1, pp. 1–16, 2021.
- [13] J. Yu, X. Dong, Q. Li, J. Lü, and Z. Ren, "Fully adaptive practical time-varying output formation tracking for high-order nonlinear stochastic multiagent system with multiple leaders," *IEEE Transactions on Cybernetics*, vol. 51, no. 4, pp. 2265–2277, 2019.
- [14] C.-L. Hwang and H. B. Abebe, "Generalized and heterogeneous nonlinear dynamic multiagent systems using online rnn-based finite-time formation tracking control and application to transportation systems," *IEEE Transactions on Intelligent Transportation Systems*, vol. 23, no. 8, pp. 13 708–13 720, 2021.
- [15] A. Azarbahram, A. Amini, and N. Pariz, "Event-triggered tracking formation of networked nonlinear intelligent transportation systems surrounded by random disturbances," *IEEE Transactions on Intelligent Transportation Systems*, vol. 23, no. 11, pp. 21 959–21 970, 2022.
- [16] F. Mehdifar, C. P. Bechlioulis, F. Hashemzadeh, and M. Baradaran, "Prescribed performance distance-based formation control of multi-agent systems," *Automatica*, vol. 119, p. 109086, 2020.
- [17] R. Babazadeh and R. Selmic, "Distance-based multiagent formation control with energy constraints using sdre," *IEEE Transactions on Aerospace and Electronic Systems*, vol. 56, no. 1, pp. 41–56, 2019.
- [18] Z. Li, H. Tnunay, S. Zhao, W. Meng, S. Q. Xie, and Z. Ding, "Bearing-only formation control with prespecified convergence time," *IEEE Transactions on Cybernetics*, vol. 52, no. 1, pp. 620–629, 2022.
- [19] K. Wu, J. Hu, B. Lennox, and F. Arvin, "Mixed controller design for multi-vehicle formation based on edge and bearing measurements," in *2022 European Control Conference (ECC)*. IEEE, 2022, pp. 1666–1671.
- [20] M. H. Trinh, D. Mukherjee, D. Zelazo, and H.-S. Ahn, "Formations on directed cycles with bearing-only measurements," *International Journal of Robust and Nonlinear Control*, vol. 28, no. 3, pp. 1074–1096, 2018.
- [21] Z. Tang, R. Cunha, T. Hamel, and C. Silvestre, "Relaxed bearing rigidity and bearing formation control under persistence of excitation," *Automatica*, vol. 141, p. 110289, 2022.
- [22] Y.-B. Bae, S.-H. Kwon, Y.-H. Lim, and H.-S. Ahn, "Distributed bearing-based formation control and network localization with exogenous disturbances," *International Journal of Robust and Nonlinear Control*, vol. 32, no. 11, pp. 6556–6573, 2022.
- [23] K. Wu, J. Hu, Z. Ding, and F. Arvin, "Finite-time fault-tolerant formation control for distributed multi-vehicle networks with bearing measurements," *IEEE Transactions on Automation Science and Engineering*, 2023.
- [24] R. Tron, J. Thomas, G. Loianno, K. Daniilidis, and V. Kumar, "A distributed optimization framework for localization and formation control: Applications to vision-based measurements," *IEEE Control Systems Magazine*, vol. 36, no. 4, pp. 22–44, 2016.
- [25] D. Zelazo, A. Franchi, and P. R. Giordano, "Rigidity theory in se (2) for unscaled relative position estimation using only bearing measurements," in *2014 European Control Conference (ECC)*, 2014, pp. 2703–2708.
- [26] S. Zhao and D. Zelazo, "Bearing rigidity and almost global bearing-only formation stabilization," *IEEE Transactions on Automatic Control*, vol. 61, no. 5, pp. 1255–1268, 2015.
- [27] X. Li, C. Wen, X. Fang, and J. Wang, "Adaptive bearing-only formation tracking control for nonholonomic multiagent systems," *IEEE Transactions on Cybernetics*, vol. 52, no. 8, pp. 7552–7562, 2021.
- [28] J. Zhao, X. Yu, X. Li, and H. Wang, "Bearing-only formation tracking control of multi-agent systems with local reference frames and constant-velocity leaders," *IEEE Control Systems Letters*, vol. 5, pp. 1–6, 2020.
- [29] K. Wu, J. Hu, B. Lennox, and F. Arvin, "Finite-time bearing-only formation tracking of heterogeneous mobile robots with collision avoidance," *IEEE Transactions on Circuits and Systems II: Express Briefs*, vol. 68, no. 10, pp. 3316–3320, 2021.
- [30] Y. Yang and W. Hu, "Containment control of double-integrator multi-agent systems with time-varying delays," *IEEE Transactions on Network Science and Engineering*, vol. 9, no. 2, pp. 457–466, 2021.
- [31] K. Aryankia and R. R. Selmic, "Neuro-adaptive formation control and target tracking for nonlinear multi-agent systems with time-delay," *IEEE Control Systems Letters*, vol. 5, no. 3, pp. 791–796, 2020.
- [32] Y. Kang, D. Luo, B. Xin, J. Cheng, T. Yang, and S. Zhou, "Robust leaderless time-varying formation control for nonlinear unmanned aerial vehicle swarm system with communication delays," *IEEE Transactions on Cybernetics*, vol. 53, no. 9, pp. 5692–5705, 2023.
- [33] Y. Hua, X. Dong, Q. Li, and Z. Ren, "Distributed fault-tolerant time-varying formation control for second-order multi-agent systems with actuator failures and directed topologies," *IEEE Transactions on Circuits and Systems II: Express Briefs*, vol. 65, no. 6, pp. 774–778, 2017.
- [34] W. Zhao, H. Liu, K. P. Valavanis, and F. L. Lewis, "Fault-tolerant formation control for heterogeneous vehicles via reinforcement learning," *IEEE Transactions on Aerospace and Electronic Systems*, vol. 58, no. 4, pp. 2796–2806, 2021.
- [35] Z. Yu, Y. Zhang, B. Jiang, C.-Y. Su, J. Fu, Y. Jin, and T. Chai, "Distributed fractional-order intelligent adaptive fault-tolerant formation-containment control of two-layer networked unmanned airships for safe observation of a smart city," *IEEE Transactions on Cybernetics*, vol. 52, no. 9, pp. 9132–9144, 2021.

- [36] C. Godsil and G. F. Royle, *Algebraic graph theory*. Springer Science & Business Media, 2013, vol. 207.
- [37] S. Zhao and D. Zelazo, "Localizability and distributed protocols for bearing-based network localization in arbitrary dimensions," *Automatica*, vol. 69, pp. 334–341, 2016.
- [38] Y.-H. Su and A. Lanzon, "Formation-containment tracking and scaling for multiple quadcopters with an application to choke-point navigation," in *2022 International Conference on Robotics and Automation (ICRA)*. IEEE, 2022, pp. 4908–4914.
- [39] S. G. Tzafestas, *Introduction to mobile robot control*. Elsevier, 2013.
- [40] G. Guo, P. Li, and L.-Y. Hao, "A new quadratic spacing policy and adaptive fault-tolerant platooning with actuator saturation," *IEEE Transactions on Intelligent Transportation Systems*, vol. 23, no. 2, pp. 1200–1212, 2020.
- [41] X. Yao, S. Li, and X. Li, "Composite adaptive anti-disturbance fault tolerant control of high-speed trains with multiple disturbances," *IEEE Transactions on Intelligent Transportation Systems*, vol. 23, no. 11, pp. 21 799–21 809, 2022.
- [42] B. Zhang, S. Lu, and W. Xie, "Cooperative game-based driver assistance control for vehicles suffering actuator faults," *IEEE Transactions on Intelligent Transportation Systems*, vol. 23, no. 7, pp. 8114–8125, 2021.
- [43] J. Wu, C. Luo, Y. Luo, and K. Li, "Distributed uav swarm formation and collision avoidance strategies over fixed and switching topologies," *IEEE Transactions on Cybernetics*, vol. 52, no. 10, pp. 10 969–10 979, 2021.
- [44] X. Dong, Y. Hua, Y. Zhou, Z. Ren, and Y. Zhong, "Theory and experiment on formation-containment control of multiple multirotor unmanned aerial vehicle systems," *IEEE Transactions on Automation Science and Engineering*, vol. 16, no. 1, pp. 229–240, 2018.
- [45] Y. Ma, B. Jiang, J. Wang, and J. Gong, "Adaptive fault-tolerant formation control for heterogeneous uavs-ugvs systems with multiple actuator faults," *IEEE Transactions on Aerospace and Electronic Systems*, vol. 59, no. 5, pp. 6705–6716, 2023.
- [46] J. Guo, Z. Liu, Y. Song, C. Yang, and C. Liang, "Research on multi-uav formation and semi-physical simulation with virtual structure," *IEEE Access*, vol. 11, pp. 126 027–126 039, 2023.
- [47] S. Zhao, Z. Li, and Z. Ding, "Bearing-only formation tracking control of multiagent systems," *IEEE Transactions on Automatic Control*, vol. 64, no. 11, pp. 4541–4554, 2019.
- [48] C. P. Chen, G.-X. Wen, Y.-J. Liu, and F.-Y. Wang, "Adaptive consensus control for a class of nonlinear multiagent time-delay systems using neural networks," *IEEE Transactions on Neural Networks and Learning Systems*, vol. 25, no. 6, pp. 1217–1226, 2014.
- [49] K. D. Young, V. I. Utkin, and U. Ozguner, "A control engineer's guide to sliding mode control," *IEEE transactions on control systems technology*, vol. 7, no. 3, pp. 328–342, 1999.
- [50] Z. Li, Z. Duan, W. Ren, and G. Feng, "Containment control of linear multi-agent systems with multiple leaders of bounded inputs using distributed continuous controllers," *International Journal of Robust and Nonlinear Control*, vol. 25, no. 13, pp. 2101–2121, 2015.



**Kefan Wu** received B.Sc degree in Applied Mathematics from Lanzhou University in 2016, M.Sc degree in Applied Mathematics from Wuhan University in 2019, and Ph.D degree in Electrical and Electronic Engineering from the University of Manchester in 2023. His research interests include networked control systems and swarm robotics.



**Junyan Hu** received B.Eng degree in Automation from Hefei University of Technology in 2015 and Ph.D degree in Electrical and Electronic Engineering from the University of Manchester in 2020.

Dr. Hu is currently an Assistant Professor in Robotics with the Department of Computer Science, Durham University. Prior to that, he worked as a Lecturer at University College London and a Postdoctoral Research Associate at the University of Manchester. His research interests include swarm intelligence, multi-agent systems, cooperative path planning, distributed control, with applications to autonomous vehicles and robotics. He serves as an Associate Editor for IEEE Robotics and Automation Letters, and a Conference Editorial Board member for ICRA and CCTA.



**Zhenhong Li** received the B.Eng. degree in electrical engineering from the Huazhong University of Science and Technology, Wuhan, China, and the M.S. and Ph.D. degrees in control engineering from the University of Manchester, Manchester, U.K., in 2014 and 2019, respectively. From 2019–2023, he was a Research Fellow at the University of Leeds. He is currently a Lecturer in Robotics and Control with the Department of Electrical and Electronic Engineering, University of Manchester, Manchester, U.K. His research interests include distributed optimization, and cooperative control of multiagent systems.



**Zhengtao Ding** received the B.Eng. degree from Tsinghua University, Beijing, China, in 1984, and the M.Sc. degree in systems and control, and the Ph.D. degree in control systems from the University of Manchester Institute of Science and Technology, Manchester, U.K. in 1986 and 1989, respectively.

After working in Singapore for ten years, he joined The University of Manchester in 2003, where he is currently a Professor in control systems and the Head of the Control, Robotics and Communication Division. He is the author of the book *Nonlinear and Adaptive Control Systems* (IET, 2013) and has published over 300 research articles. His research interests include nonlinear and adaptive control theory and their applications, more recently network-based control, distributed optimization and distributed learning, with applications to power systems and robotics. He is a fellow of The Alan Turing Institute. He serves/has served as the Editor-in-Chief for Drones and Autonomous Vehicles, the Subject Chief Editor for Frontiers, and an Associate Editor for IEEE Transactions on Automatic Control, IEEE Control Systems Letters, and several other journals.



**Farshad Arvin** received the BSc degree in Computer Engineering, the MSc degree in Computer Systems engineering, and the PhD degree in Computer Science, in 2004, 2010, and 2015, respectively. Farshad is an Associate Professor in Robotics in the Department of Computer Science at Durham University in UK. Prior to that, he was a Senior Lecturer in Robotics at The University of Manchester, UK. He visited several leading institutes including Artificial Life Laboratory at the University of Graz, Institute of Microelectronics, Tsinghua University,

Beijing, and Italian Institute of Technology (iit) in Genoa as a Senior Visiting Research Scholar. His research interests include swarm robotics and autonomous multi-agent systems. He serves as an Associate Editor for IEEE Transactions on Cognitive and Developmental Systems. He is the Founding Director of the Swarm & Computation Intelligence Laboratory formed in 2018, [www.SwaCIL.com](http://www.SwaCIL.com).



**Citation on deposit:** Wu, K., Hu, J., Li, Z., Ding, Z., & Arvin, F. (2024). Distributed Collision-Free Bearing Coordination of Multi-UAV Systems With Actuator Faults and Time Delays. *IEEE Transactions on Intelligent Transportation Systems*, 1-14.

<https://doi.org/10.1109/tits.2024.3364356>

**For final citation and metadata, visit Durham Research Online URL:**

<https://durham-repository.worktribe.com/output/2379781>

**Copyright statement:** This accepted manuscript is licensed under the Creative Commons Attribution 4.0 licence.

<https://creativecommons.org/licenses/by/4.0/>